WSRC-TR-2001-00591 Rev 0
SRT-RPP-2001-00227 Rev 0

DESIGN ANALYSIS FOR A SCALED EROSION TEST

UNCLASSIFIED
DOES NOT CONTAIN
UNCLASSIFIED CONTROLLED
NUCLEAR INFORMATION

ADC &
Reviewing
Official: ______________________
(Name and Title)

Date:______________________

Westinghouse Savannah River Company
Savannah River Site
Aiken, SC 29808

SAFETY • RESPONSIBILITY • SECURITY
SRS
SAVANNAH RIVER SITE

Prepared for the U.S. Department of Energy under Contract No. DE-AC09-96SR18500

This document was prepared in conjunction with work accomplished under Contract No. DE-AC09-96SR18500 with the U.S. Department of Energy.

WSRC-TR-2001-00591
SRT-RPP-2001-00227

KEYWORDS:
Hanford River Protection Project
Computational Approach
Erosion Model
Particle Impingement Model

DESIGN ANALYSIS FOR A SCALED EROSION TEST

SAVANNAH RIVER TECHNOLOGY CENTER

Si Young Lee and Richard A. Dimenna

April 2002

Westinghouse Savannah River Company
Savannah River Site
Aiken, SC 29808

Prepared for the U.S. Department of Energy under Contract No. DE-AC09-96SR18500

WSRC-TR-2001-00591
SRT-RPP-2001-00227

(This Page Intentionally Left Blank)

DOCUMENT:WSRC-TR-2001-00591 (SRT-RPP-2001-00227)

TITLE: DESIGN ANALYSIS FOR A SCALED EROSION TEST

APPROVALS

____ Date:____________

Si Y. Lee, Author (EM&S Group/ SRTC)

____ Date:____________

Richard A. Dimenna, Co-Author (EM&S Group/ SRTC)

____ Date:____________

Reid A. Peterson, RPP-WTP (WGI)

____ Date:____________

Cynthia P. Holding-Smith, Manager (EM&S Group/SRTC)

____ Date:____________

Steve T. Wach, Manager (EDS/SRTC)

____ Date:____________

Hector N. Guerrero, Technical Reviewer (EDS/SRTC)

(This Page Intentionally Left Blank)

Table of Contents

(This Page Intentionally Left Blank)

List of Figures

List of Tables

(This Page Intentionally Left Blank)

Nomenclature

A = area (ft^2 or m^2)

C = solid volume concentrations in slurry (--)

d = branch diameter or solid particle size in slurry (ft or m)

D = main pipe diameter (ft or m)

f = empirical factor

F = Force (N)

g = gravity (m/sec^2)

I = turbulence intensity (--)

k = constant in eq. (2) (--)

m = particle mass flowrate (kg/sec)

P = pressure (Pa)

Pr = Prandtl number, $\mu C_p/k$, (--)

R = curvature radius of elbow (ft or m)

Re = Reynolds number, $d\rho u/\mu$

t = time (second)

U = slurry velocity (ft/sec or m/sec)

u = component velocity in x-direction (ft/sec or m/sec)

u' = local turbulent velocity fluctuation in x-direction (ft/sec or m/sec)

v = local flow velocity or component velocity in y-direction (ft/sec or m/sec)

v' = local turbulent velocity fluctuation in y-direction (ft/sec or m/sec)

V = average velocity magnitude (ft/sec or m/sec)

W = weight fraction of solids in slurry (--)

w = component velocity in z-direction (ft/sec or m/sec)

w' = local turbulent velocity fluctuation in z-direction (ft/sec or m/sec)

x = local position along the x-direction under Cartesian coordinate system (ft or m)

y = local position along the y-direction under Cartesian coordinate system (ft or m)

z = local position along the y-direction under Cartesian coordinate system (ft or m)

Greek

ρ = density (kg/m^3)

β = impingement angle of particle against wall surface

κ = turbulent kinetic energy (= $\frac{1}{2}\left(u'^2 + v'^2 + w'^2\right)_{avg}$)

ε = rate of dissipation of turbulent kinetic energy

Δ = difference

∇ = gradient operator

μ = dynamic viscosity (N sec/m^2)

ν = kinematic viscosity (m^2/sec)

ξ = empirical facto for erosion rate

Subscript

avg = average

c = critical

d = incident particle

f = fluid

in = incidence

p = particle

s = solid particle

t = turbulent

wall = wall surface

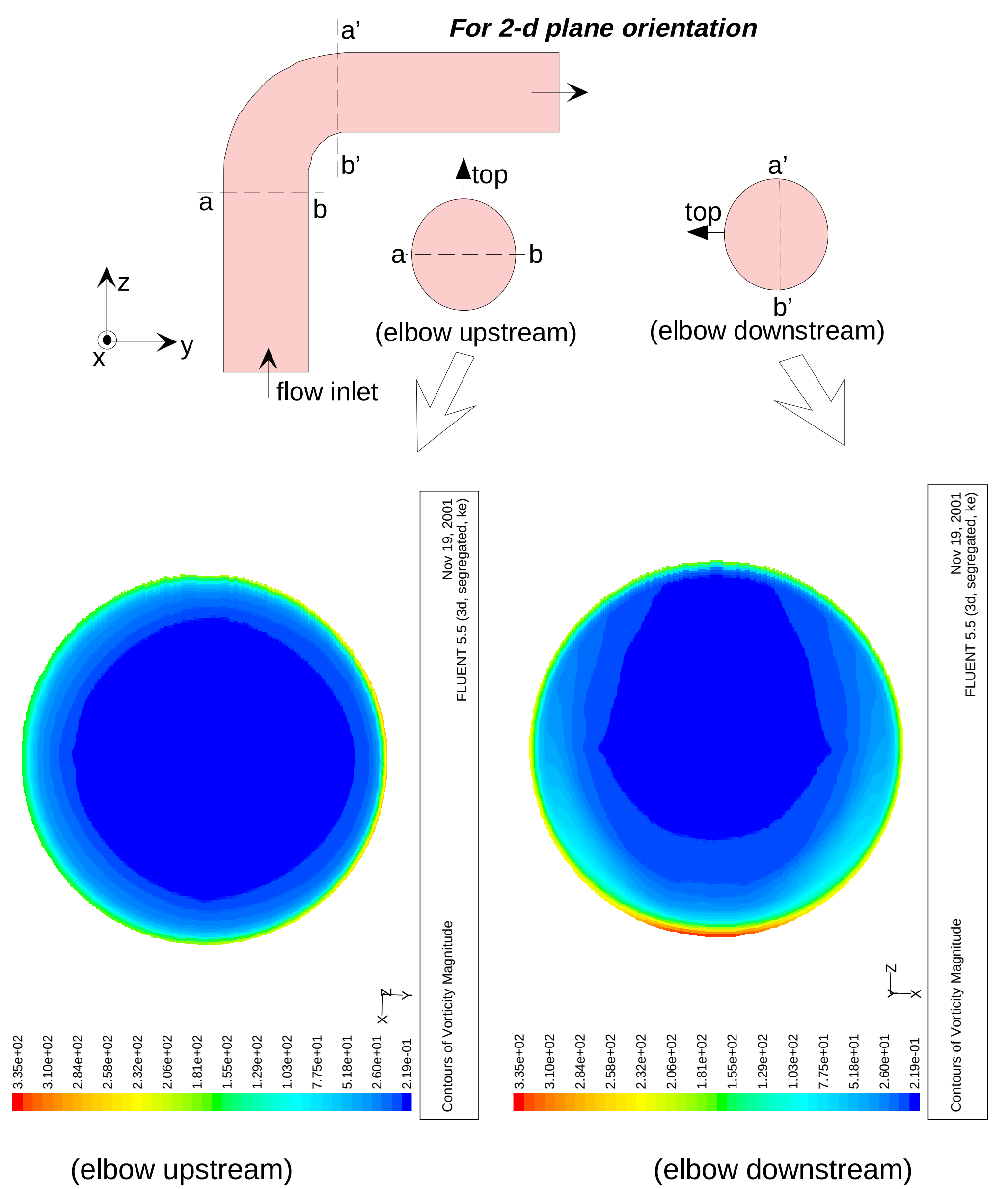

Figure 17. Vorticity magnitudes at the cross-sectional planes of the upstream and downstream regions of the elbow component.

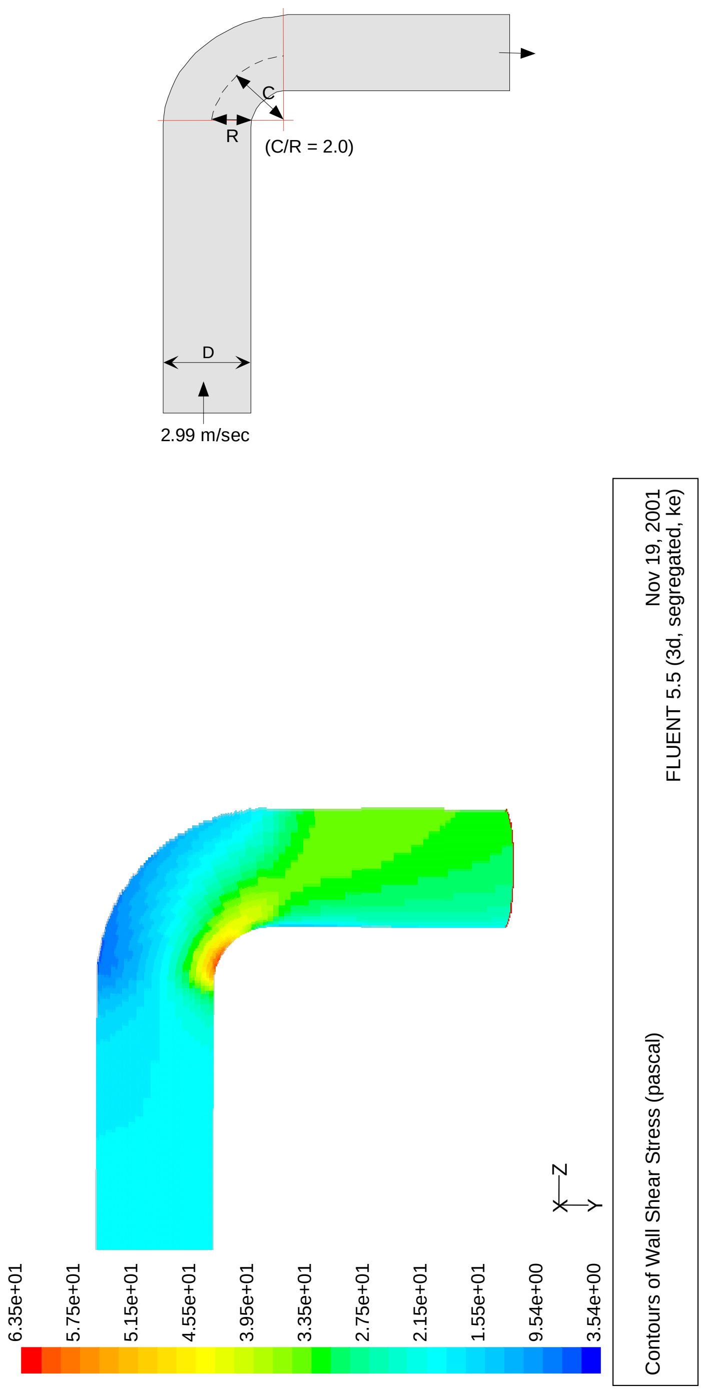

Figure 18. Wall shear stress distributions for a slurry flow in isolated elbow.

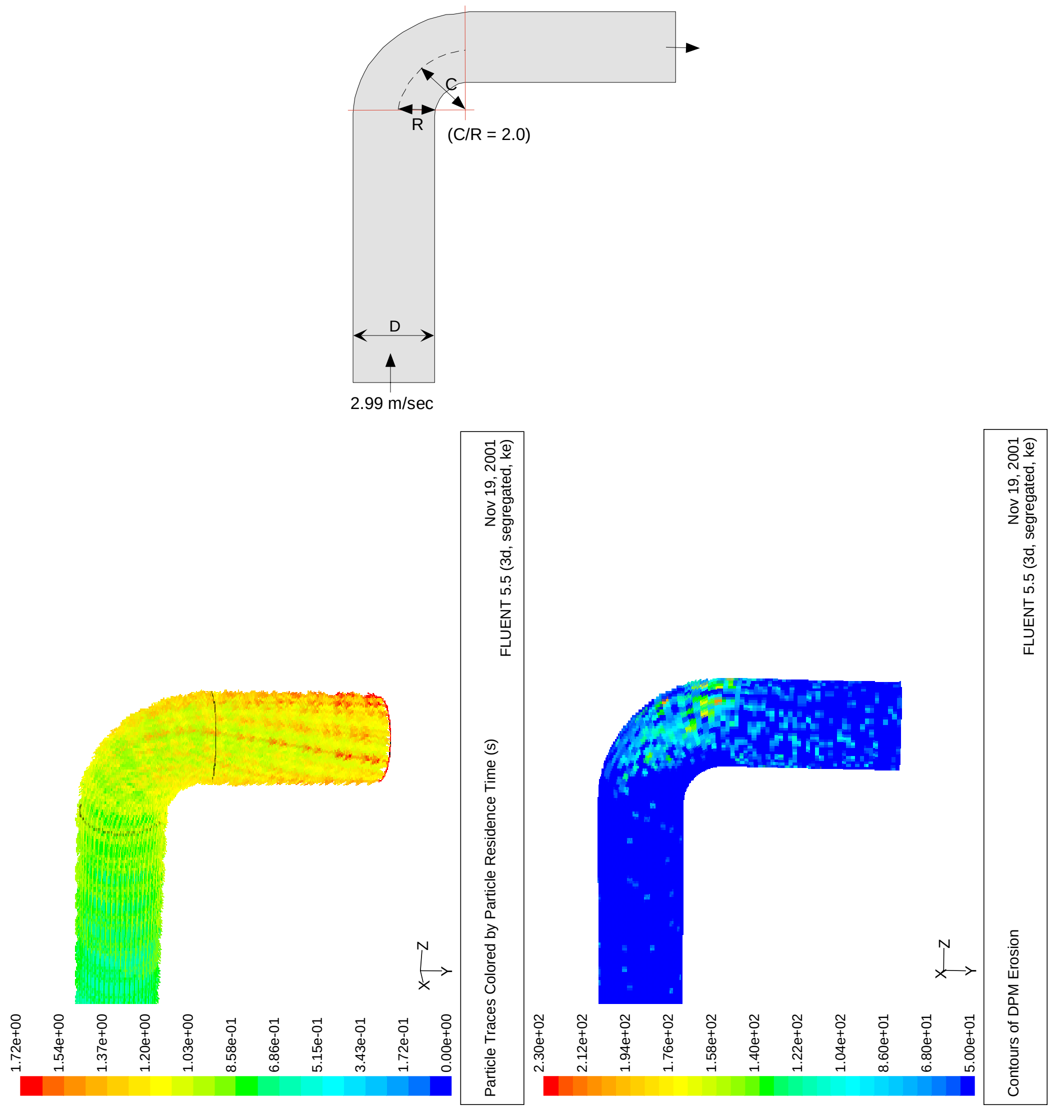

(particle trajectory) (erosion distributions)

Figure 19. Particle trajectory and erosion distributions due to the impingement of particles in a slurry.

Table 6. Maximum shear stresses and relative maximum erosion for the elbows with different curvature

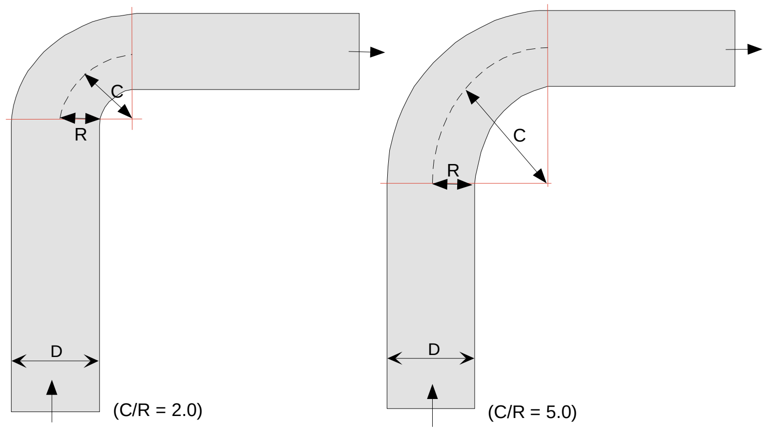

Elbow Curvature (C/R)	2.0	5.0
Flowrate	2400 gpm	2400 gpm
Elbow Diameter	10in	10in
Max. Wall Shear	67.2 Pa	31.6 Pa
Relative scale for erosion rate	1.0	~0.65

Table 7. Maximum wall shear stresses for the cases considered in the analysis associated with erosion (D = 10 in and d= 3 in)

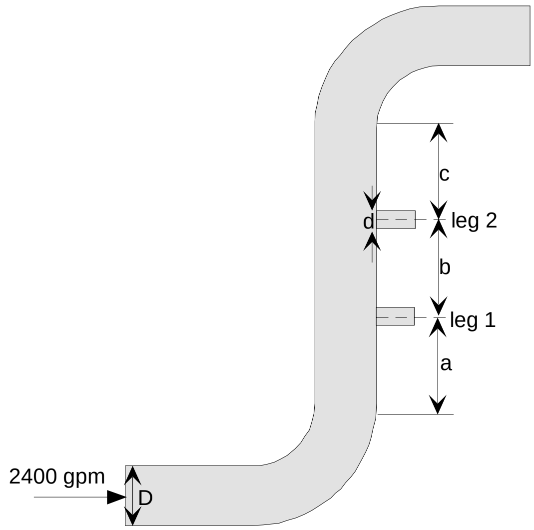

Cases (Fig. 4)	Case-b	Case-c					Case-d
Presence (?) of elbows at the downstream and upstream regions of the 10" pipe	Yes	Yes	Yes	Yes	Yes	Yes	No (10in diameter and 36in long pipe)
Number of legs	2	1(leg 1)	1(leg 2)	1(leg1)	1(leg1)	1(leg1)	1 (leg 1)
Total length between elbows	36in	36in	36in	33in	30in	72in	36in
a	12in	12in	12in	9in	9in	9in	12in
b	12in	12in	12in	12in	12in	12in	--
c	12in	12in	12in	12in	9in	51in	--
Max. wall shear (Pa)	62.6	63.7	63.2	64.7	66.2	62.9	40

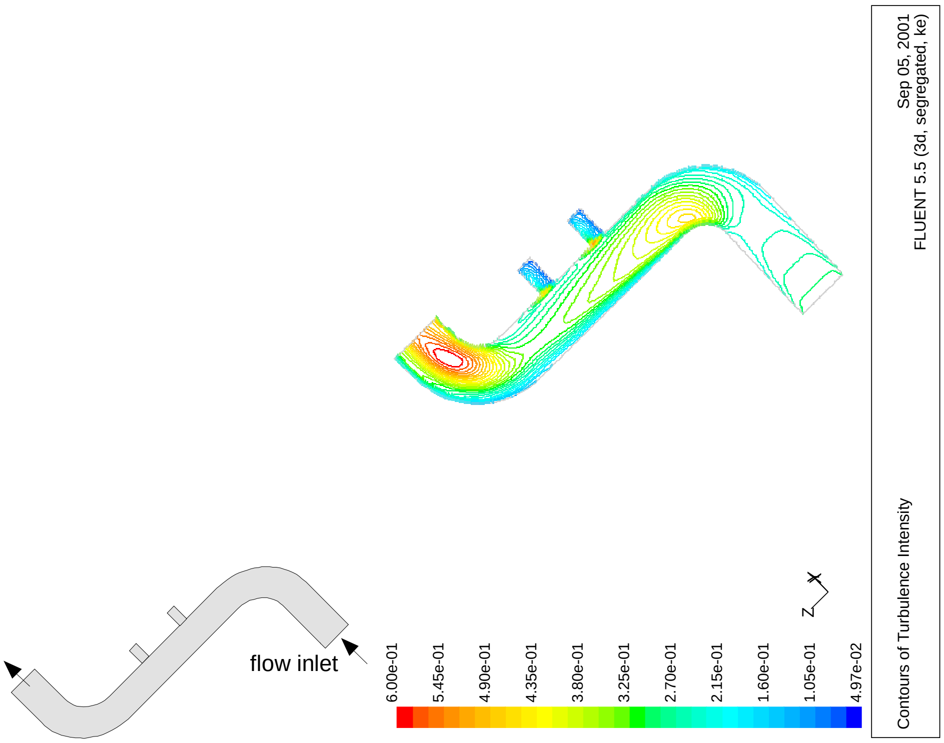

(Case b in Fig 4)

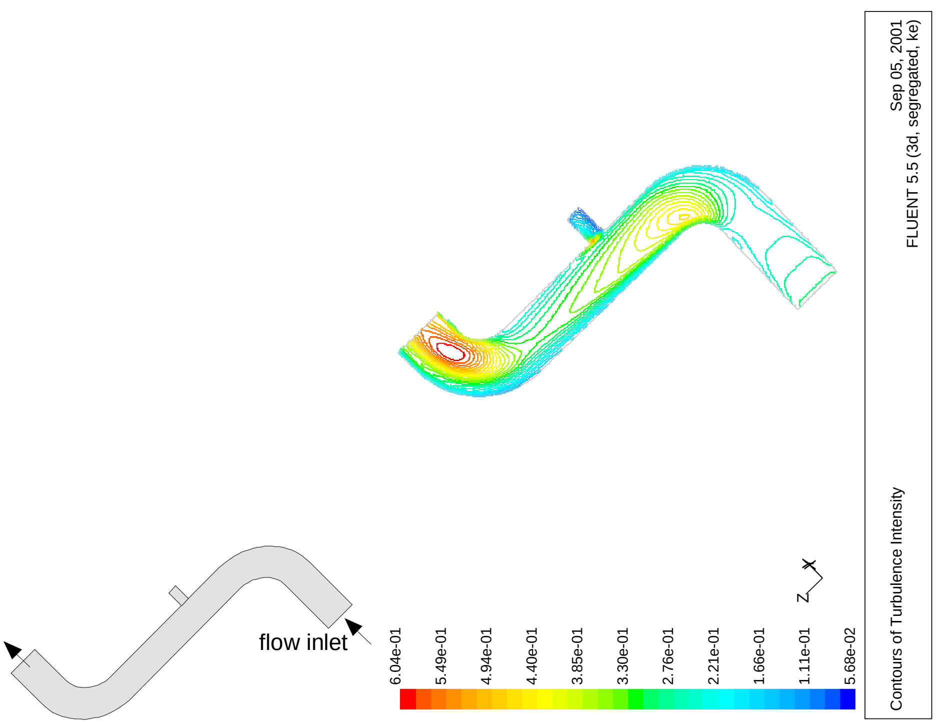

(Case c in Fig. 4)

Figure 20. Comparison of turbulence intensity for two cases associated with particle dispersion.

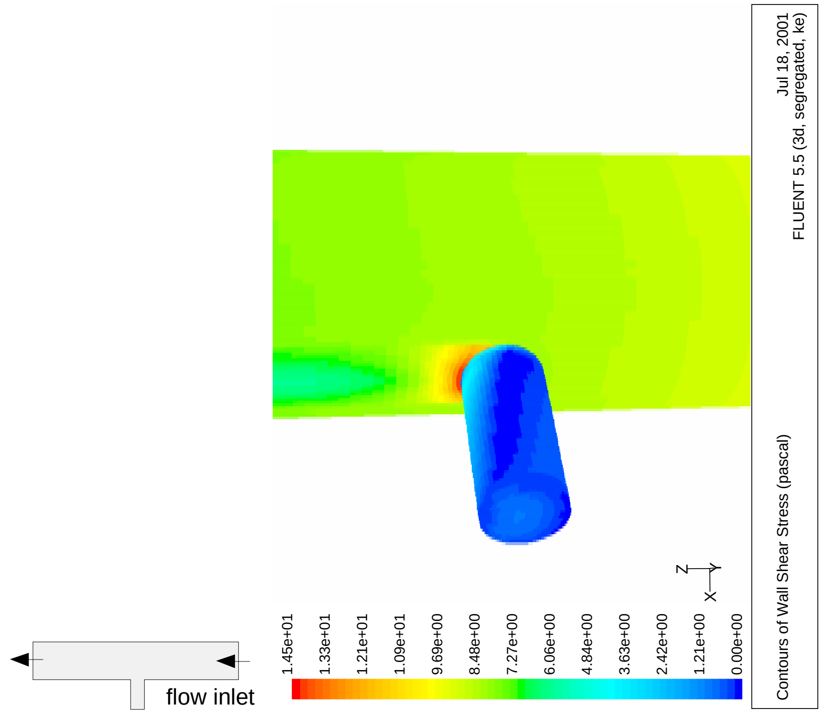

(Wall shear distributions)

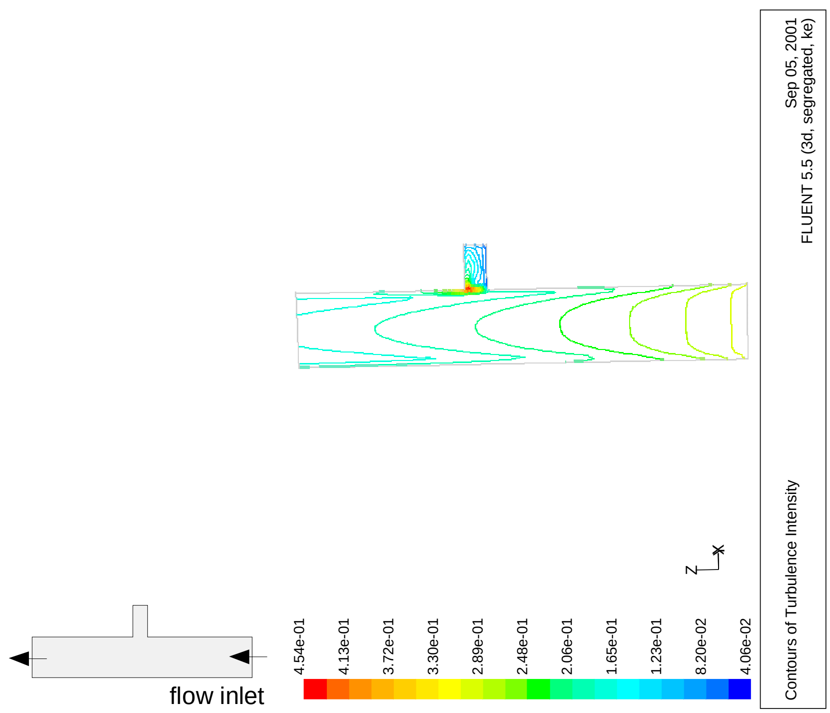

(Turbulence intensity distribution at the center-plane)

Figure 21. Wall shear stress and turbulence intensity distributions for the 36 in long and 10 in diameter pipe with 3in leg (case g) associated with wall erosion.

Table 8. Maximum wall shear stresses for the models of the filter component associated with erosion (filter tube diameter = 0.5 in)

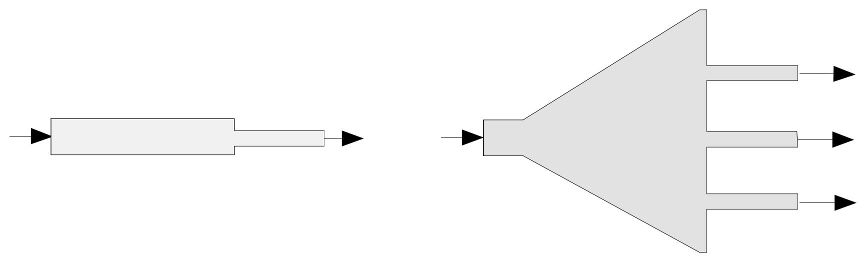

(One-tube equivalent filter model) (7-tube equivalent filter model)

Cases	One-tube equivalent model (case-e in Fig. 4)	Seven-tube equivalent model (case-g in Fig. 4)
Filter geometry	One tube	7 tube
Filter tube diameter	0.5in	0.50in
Filter boundary diameter	7/8in	4in
Max. wall shear	185.2 Pa	171.5 Pa
Max. erosion location due to impingement	Upstream tube sheet (see Fig. 25)	Upstream tube sheet (see Fig. 25)
Relative scale for erosion	1.0	~0.7

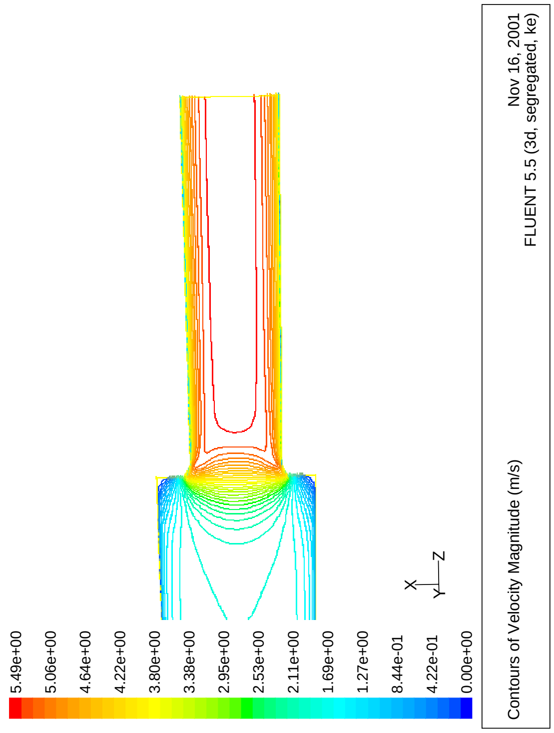

(Velocity contour at the center plane of smooth filter tube)

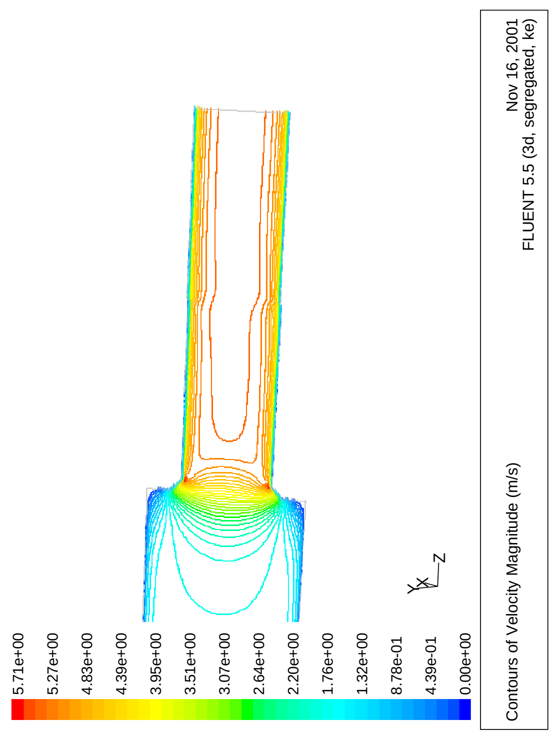

(Velocity contour at the center plane of welded filter tube)

Figure 22. Comparison of velocity distributions at the center planes of the one-tube models with smooth and welded tubes (case-e and case-f in Fig. 4).

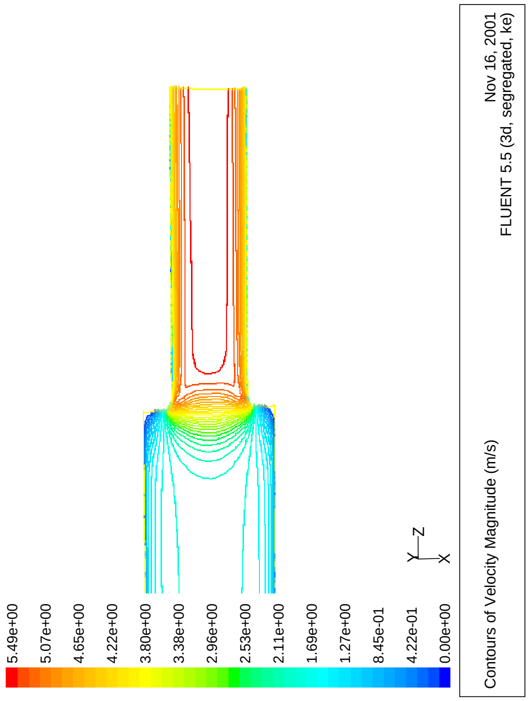

(one-tube filter model)

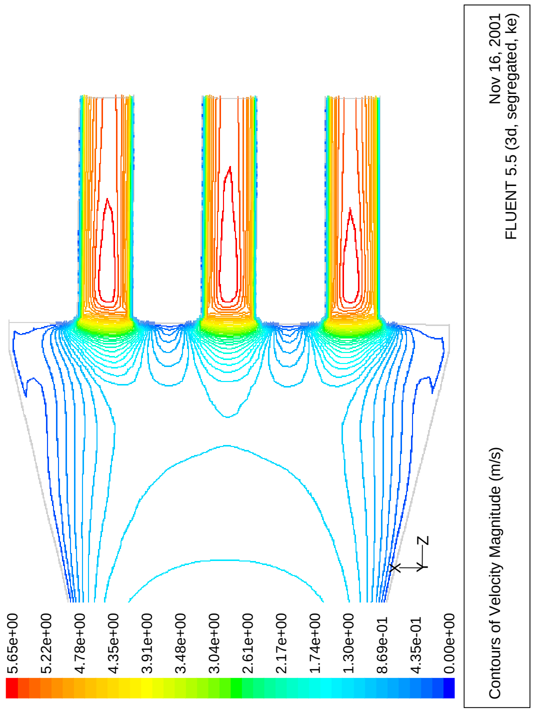

(7-tube filter model)

Figure 23. Comparison of velocity distributions at the center plane of the one-tube and seven-tube filter models to simulate the cross-flow filtration component.

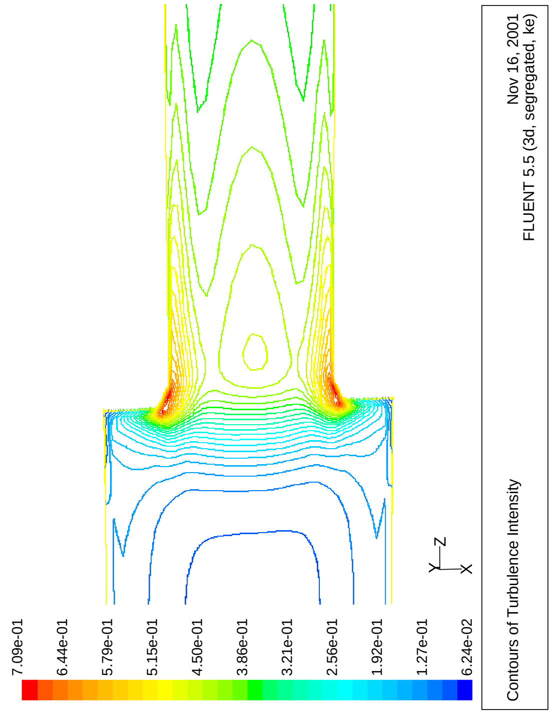

(one-tube filter model)

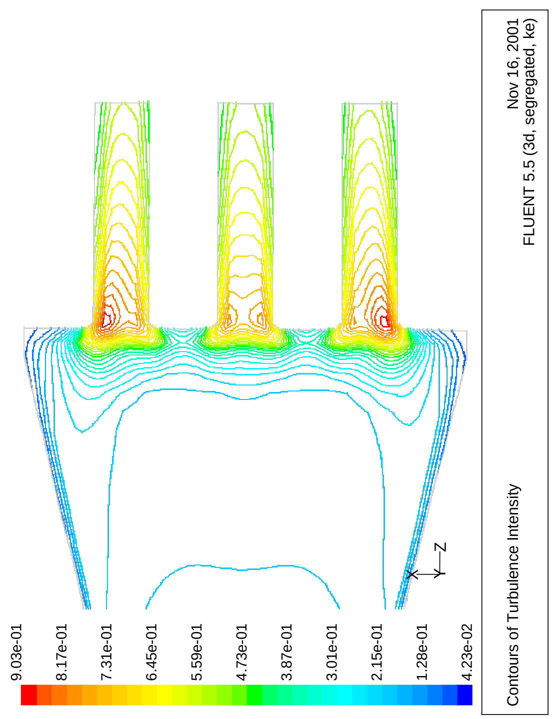

(7-tube filter model)

Figure 24. Comparison of turbulence intensity distributions at the center plane of the one-tube and seven-tube filter models to simulate the cross-flow filtration component using flow domains and conditions shown in Figs. 7 and 8.

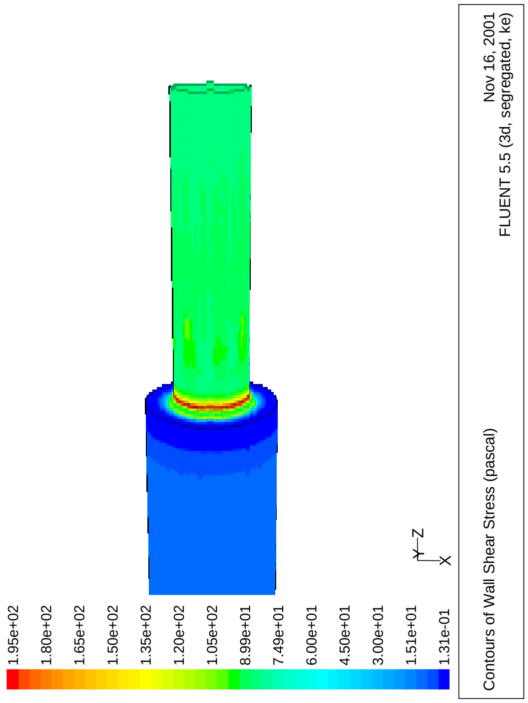

(Wall shear distributions for the one-tube model)

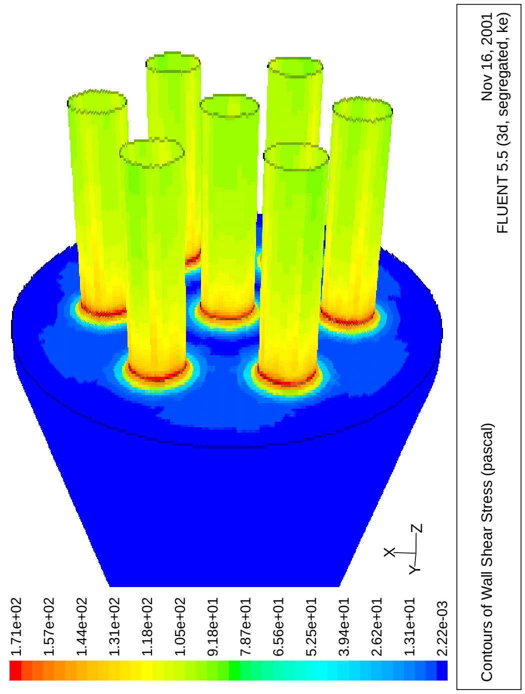

(Wall shear distributions for the 7-tube model)

Figure 25. Comparison of wall shear distributions between one-tube model and 7-tube model to simulate the cross-flow filtration system.

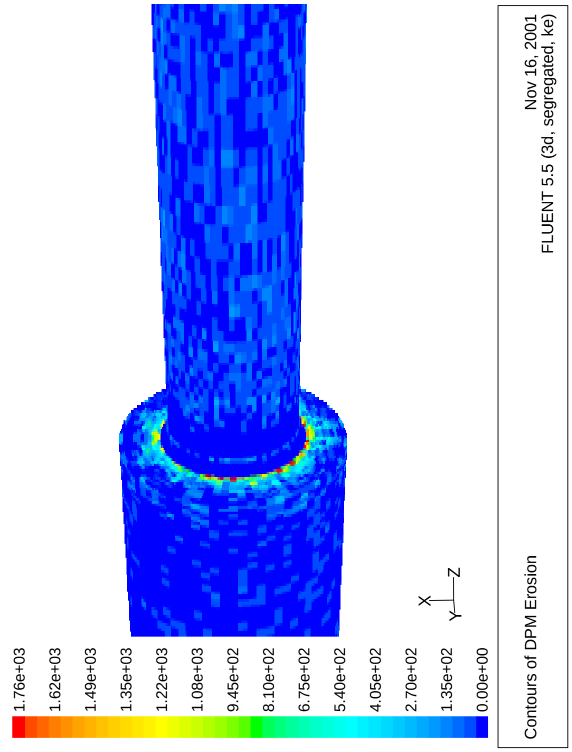

(one-tube filter model representing the case-e geometry)

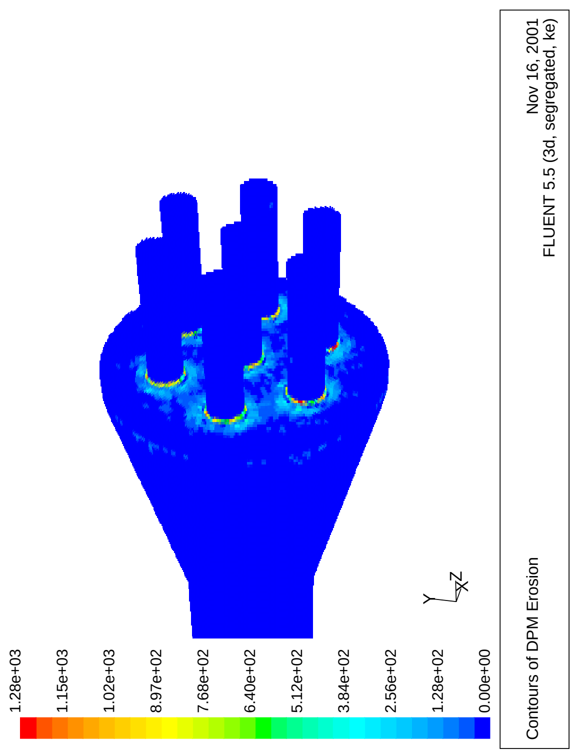

(seven-tube filter model representing the case-g geometry)

Figure 26. Comparison of erosion distributions for the two filter models.

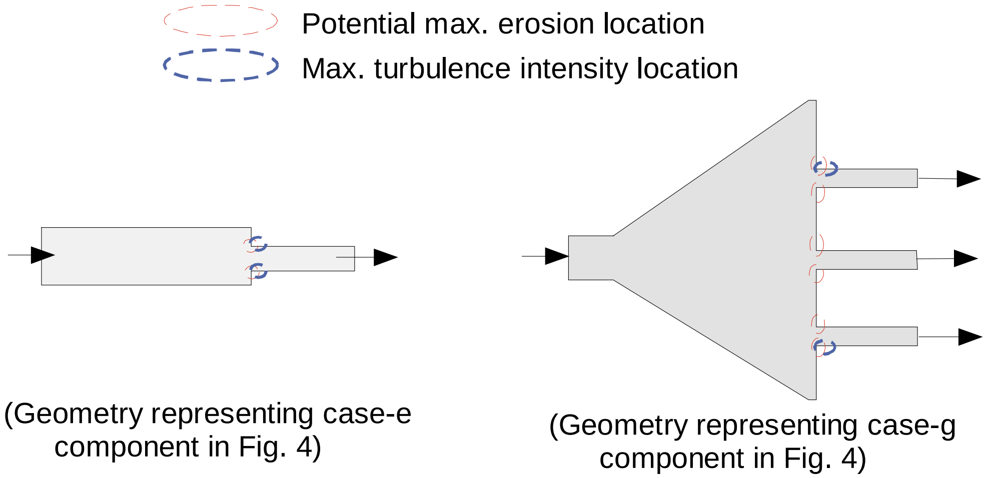

Figure 27. Potential maximum erosion locations at the middle planes of one-tube (case-e) and seven-tube filter (case-g) components of the cross-flow filtration facility predicted by the present model.

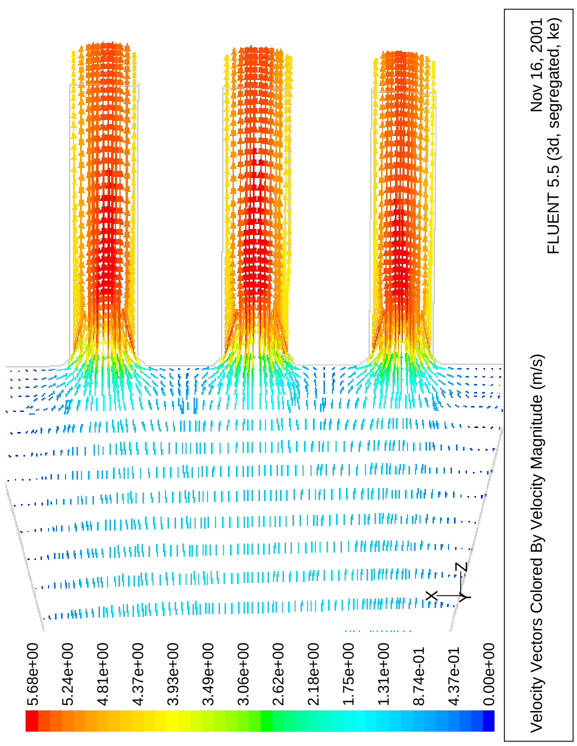

Figure 28. Velocity vector plot at the center plane of the 7-tube model.

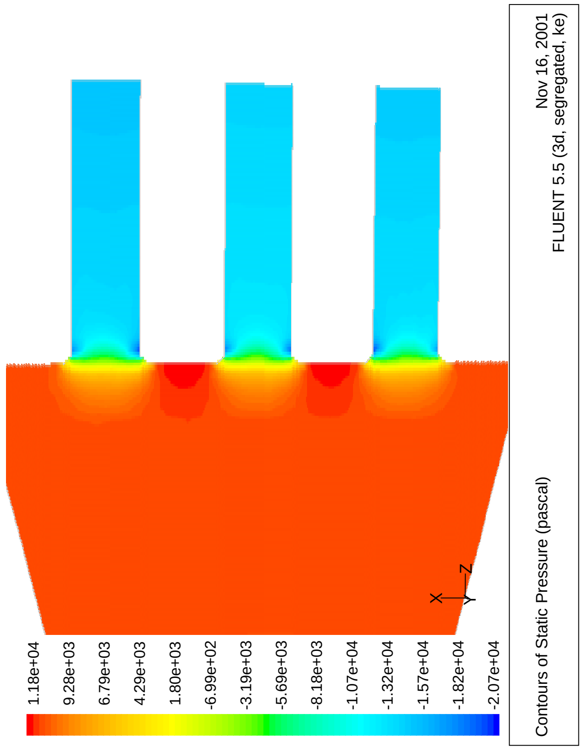

Figure 29. Pressure distributions at the center plane of the 7-tube model.

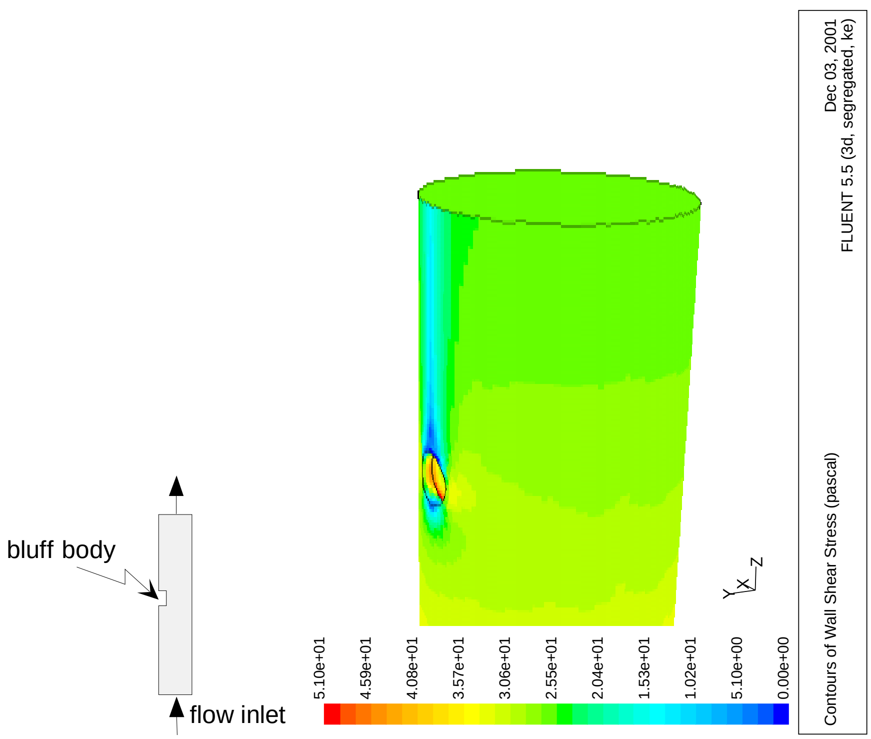

Figure 30. Wall shear distributions for the bluff body (case-i in Fig 4) predicted by the present model.

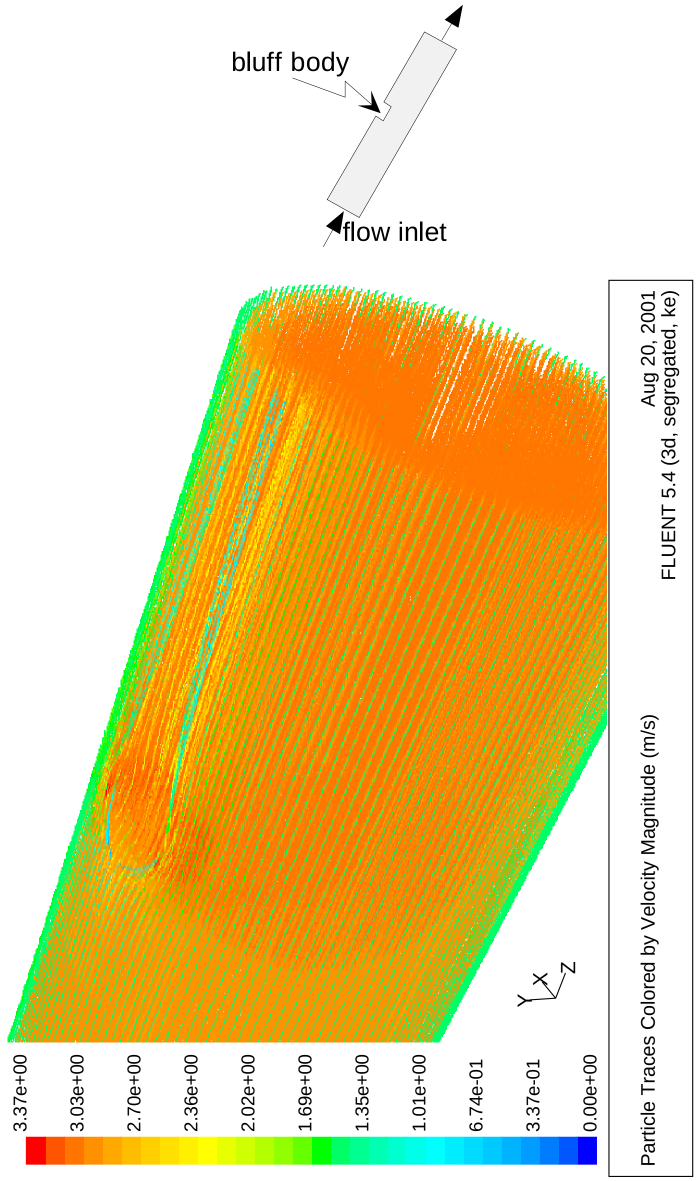

Figure 31. Particle trajectories for the bluff body inside the straight pipe (case-i in Fig 4) predicted by the particle impingement model.

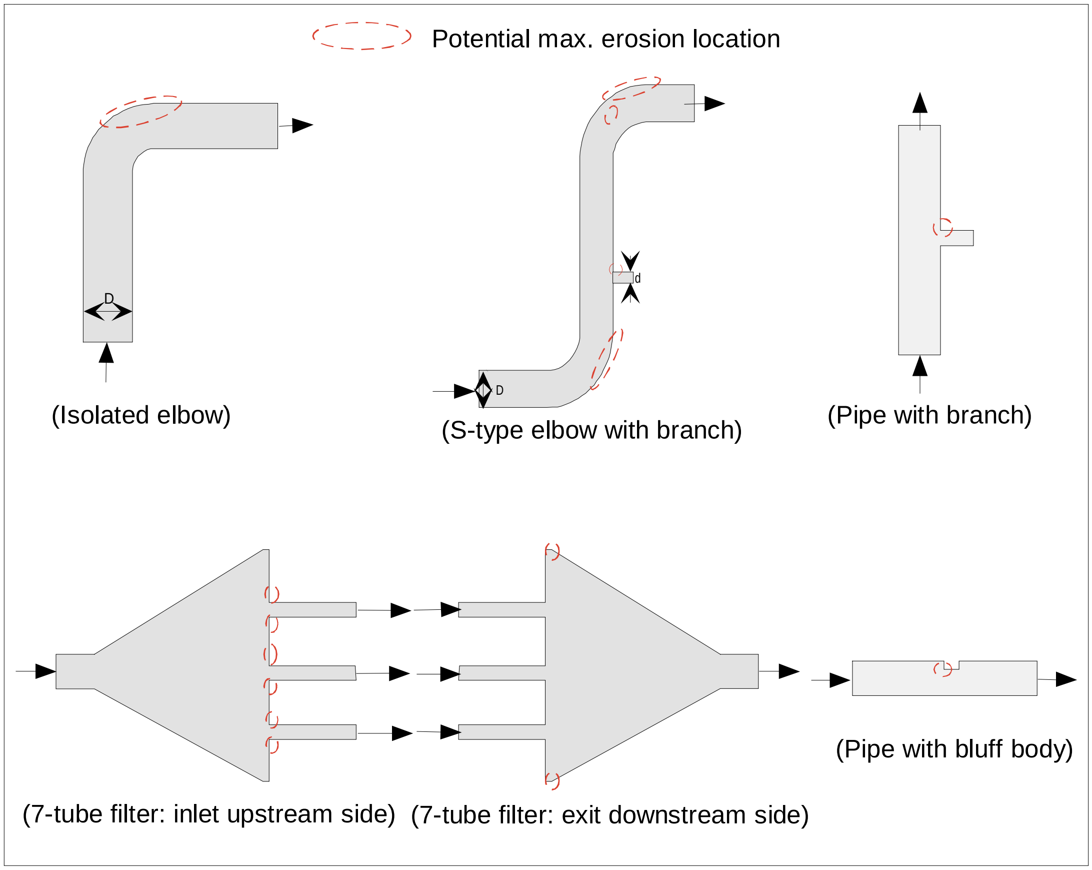

Figure 32. Potential maximum erosion locations at the middle planes of key components of the cross-flow filtration facility selected by the present model.

Table 9. Maximum wall shears for the models of the key components considered in the analysis associated with erosion (filter tube diameter = 0.5 in)

Cases	**Isolated elbow** (case-a*)	**Two elbows with branch** (case-c*)	**7-tube filter**		**Pipe with bluff body** (case-i*)
			Inlet (case-g*)	**Exit** (case-h*)	
Max. wall shear (Pa)	72.0	66.2	171.5	115.8	51.0
Max. erosion location due to impingement (see Fig. 31)	Outer elbow	Outer elbow	Upstream tube sheet	Downstream tube sheet	Front bluff
Relative** scale for max. erosion rate	~0.4	~0.9	1.0	~0.1	~0.3

Note: * Each case is identified in Fig. 4.
** The scale is relative to the maximum erosion rate of case-g.

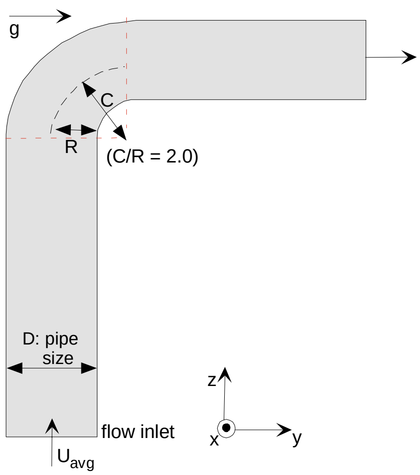

Elbow orientations

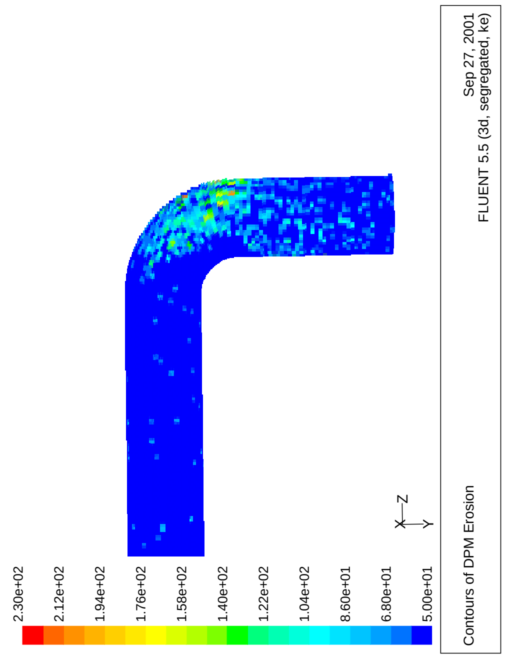

10in full-scale elbow (U_{avg} = 2.99 m/sec)

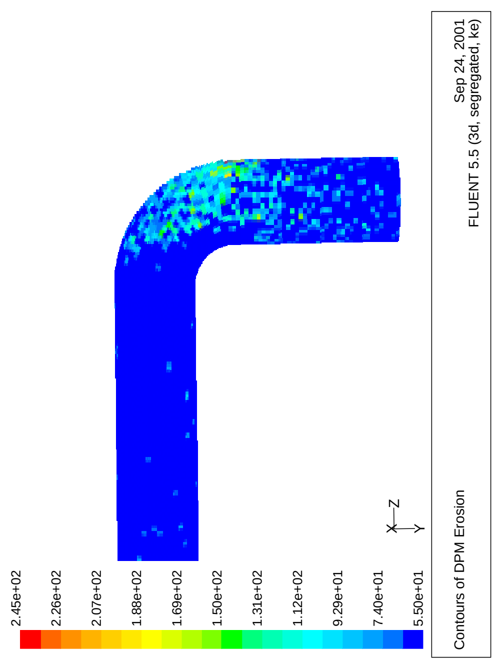

3in scaled elbow (U_{avg} = 3.5 m/sec)

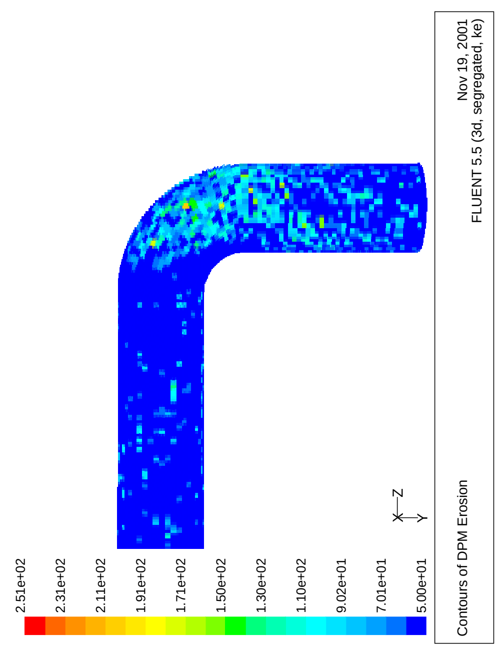

1in scaled elbow (U_{avg} = 4.0 m/sec)

Figure 33. Comparison of the erosion distributions due to particle impingement under three different scaled elbow components

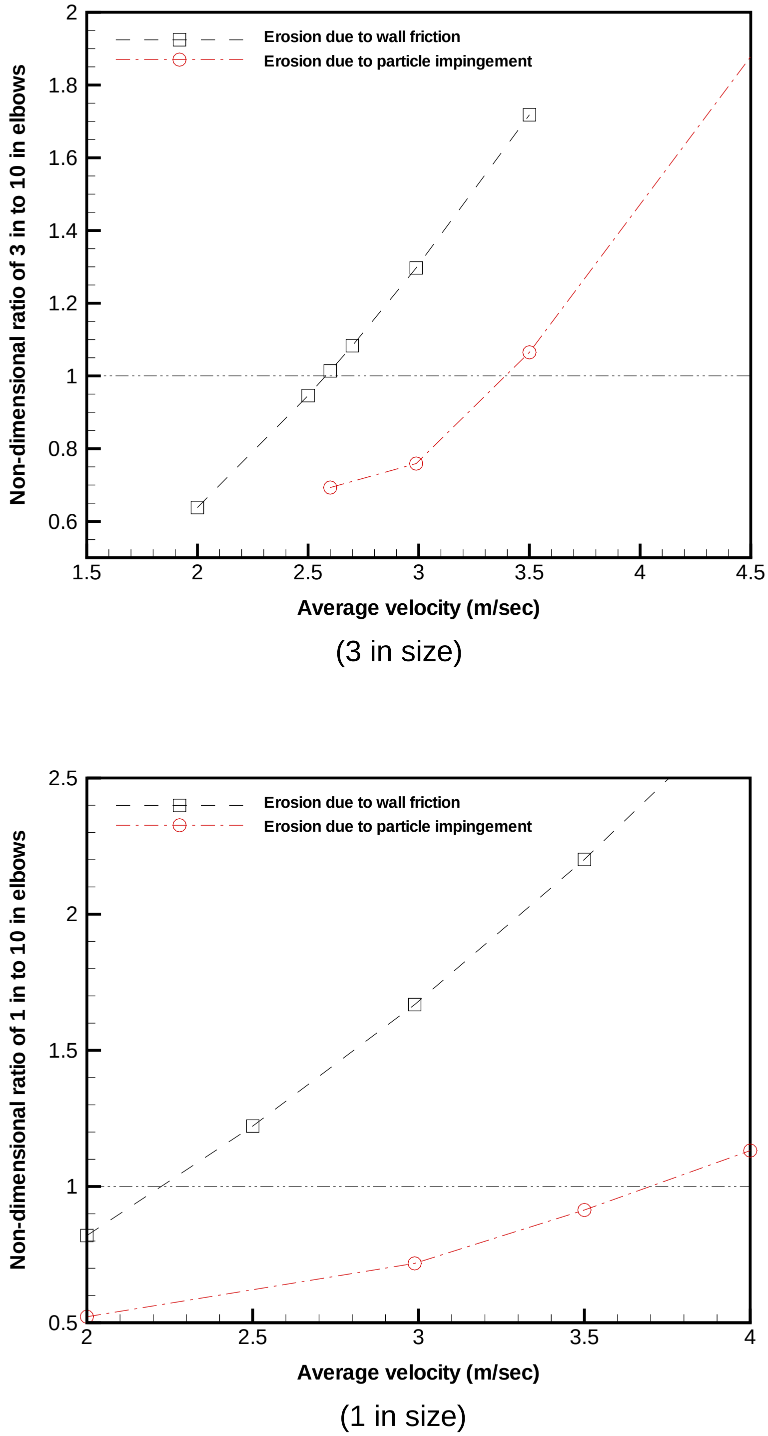

Figure 34. Nondimensional erosion ratio of scale-down (3 in and 1in) to 10 in prototypic elbow for various slurry velocities

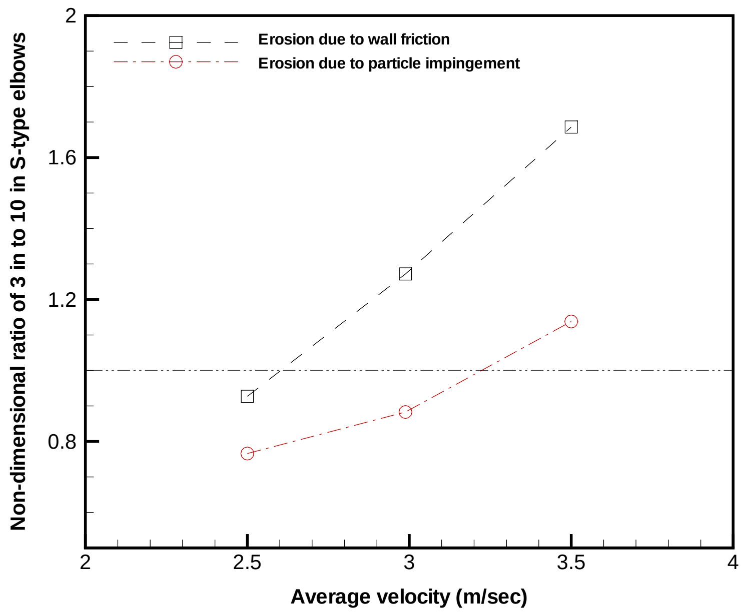

(3 in pipe size)

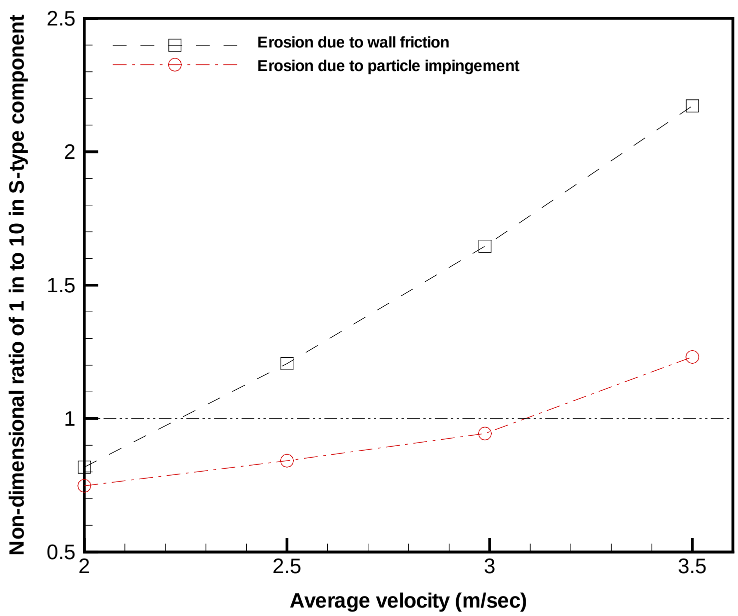

(1 in pipe size)

Figure 35. Nondimensional erosion ratio of scale-down (3 in and 1in) to 10 in prototypic S-type pipings for various slurry velocities

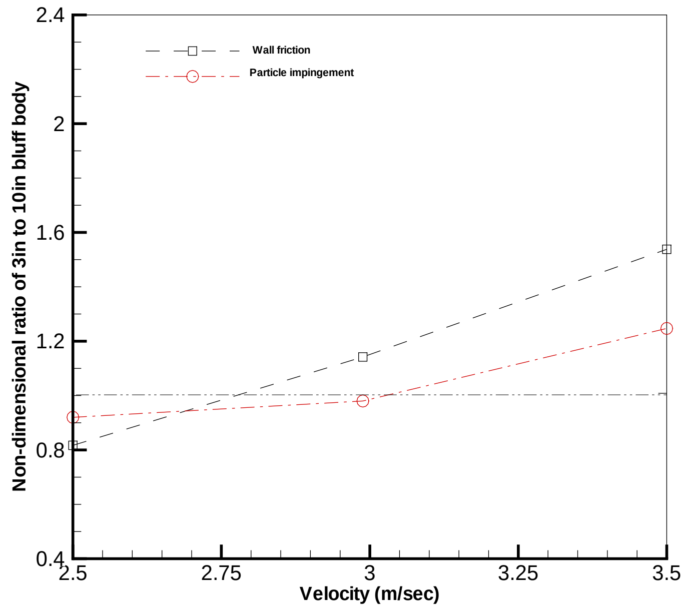

(3 in size)

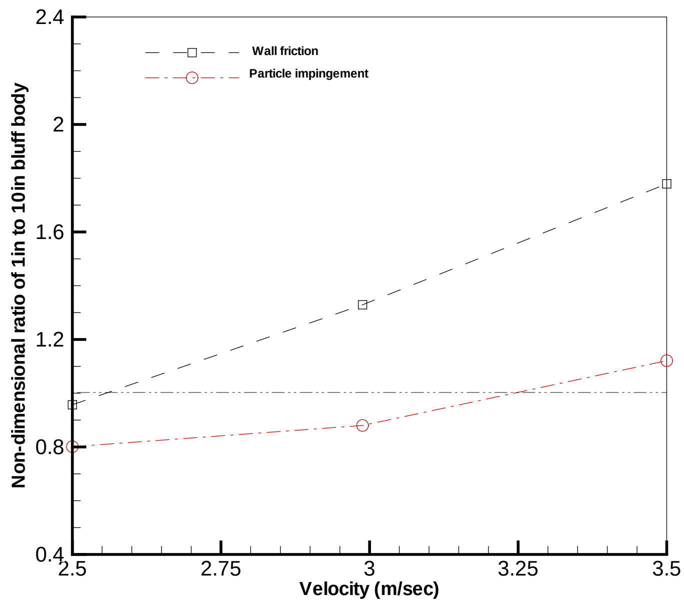

(1 in size)

Figure 36. Nondimensional erosion ratio of scale-down (3 in and 1 in) to 10 in prototypic bluff body for various slurry velocities

5. Conclusions

This report presents the application of computational fluid dynamics (CFD) methods to ensure that the test facility design would capture the erosion phenomena expected in the full-scale cross-flow ultrafiltration facility. The present models assume that there are two manners in which a wall surface is worn. The first is based on the homegeneous solid-fluid model, and its basic mechanism is that wall friction of the mixed slurry on the abraded surface can cause wear. The other is that some particles impinged on the wall surface are able to cut chips out of the impacted surface. For the present work, Eulerian continuous transport equations and Lagrangian momentum balance for the solid phase dispersed in the slurry flow were used to estimate wall shear and particle-impinged erosions. For typical operating conditions of the facility, Reynolds number is about 10^5 corresponding to fully-turbulent flow regime. Two-equation turbulence model was used to consider the dispersion effect of particles due to turbulent eddies. In the present calculations, solids content of the working fluid, the regions of high wall shear, and particle impingement with the walls were considered as major mechanisms associated with the erosion.

Three sets of representative experiments were chosen to test the CFD models presented in this work. All these tests were performed using sand-water slurry. The benchmarking results against the literature data for hydraulic transport and erosion tests are reasonably good taking into account the complex nature of fluid-solid two-phase phenomena.

The CFD analyses were then designed to characterize slurry-flow profiles, wall shear, and particle impingement distributions in key pipe bends and fittings representative of the filtration system. Pipe diameters, lengths, the locations of pipe fittings, and slurry velocities were scaled with the CFD calculations to ensure that the erosion drivers in the test facility were representative of the full-scale facility. To be conservative, the highest velocity over full-scale value (9.8 ft/sec) will be used, that is, 3.4 m/sec (11.2 ft/sec) for the 3 in test loop (14% over full-scale) and 3.7 m/sec (12.1 ft/sec) for the 1 in test loop (24% over full-scale). The results are also shown in Fig. 34.

From the present analysis results, main conclusions are drawn as follows:

- The prediction results show that when the slurry velocity increases, wall shear stress closely related to the abrasive erosion is more sensitive to the scaling of pipe size, compared to that of particle impingement behavior.
- The analysis results show that erosion decreases with increasing turbulence intensity, leading to the increased radial dispersion of slurry. This is consistent with the literature information.
- All the main loop components of the cross-flow filtration facility were studied to simplify the components without losing key erosion phenomena and slurry flow characteristics expected in the full-scale facility. Key components selected by the present analysis are isolated elbow, two-elbow connected closely with single branch, seven-tube filter arrangement, and bluff body attached to the inner wall of horizontal pipe.
- The present computational models determined operating flow conditions for the scaled test facility to ensure that the erosion behaviors expected at the full-scale

facility are properly captured in the scale-down test facility. In this case, three different component configurations were applied for the scaling considerations under three different size conditions, including 10 in prototypic scale, 3 in and 1 in test scales.

- The locations of high erosion, which were predicted by the particle impingement model for each of the selected components, provided the guidance for erosion measurement under scaled test facility.
- From the benchmarking of the present CFD models against the literature data, the model predictions agree with the test data within about 15%.

When the test results from the scaled experiment facility at SRTC are available, the present models will be benchmarked in more detail. This results in a validation of those calculations, and will allow the test results to be applied to a quantitative estimation of erosion over the entire plant lifetime of the full-scale filtration facility.

6. References

1. Duignan, M. R., "Slurry Wear Evaluation of the Pretreatment Cross-flow Filtration and Evaporation Systems", WSRC-TR-2001-00145, SRT-RPP-2001-000038, Rev. 0, October 15, 2001.
2. Duignan, M. R., "Computational Assistance for the Slurry Wear Evaluation of the Pretreatment Cross-flow Filtration and Evaporation Systems", WSRC-TR-2001-00194, SRT-RPP-2001-000041, Rev. 0, June 11, 2001.
3. Duignan, M. R. and Lee, S. Y., "RPP-WTP Slurry Wear Evaluation: Literature Review", Savannah River Technology Center, WSRC-TR-2001-00156, SRT-RPP-2001-00033, March 21, 2001.
4. Duignan, M. R. ,"RPP-WTP Slurry Wear Evaluation: Slurry Abrasivity," Savannah River Technology Center, WSRC-TR-2002-00062, SRT-RPP-2002-00022, January 31, 2002.
5. Burstein, G.T. and Sasaki, K., Effect of impact angle on the slurry erosion-corrosion of 304L stainless steel. Wear 240, 80-94, 2000.
6. Eibling, R.E. and Nash, C.A., Hanford waste simulants created to support the research and development on the River Protection Project – Waste Treatment Plant. Westinghouse Savannah River Company Report No. WSRC-TR-2000-00338, 2000.
7. Elmore, M.R., "imulant Erosion Testing", Battelle Pacific Northwest National Laboratory Report No. WTP-RPT-001, 2000.
8. Finnie, I., "Some reflections on the past and future of erosion", Wear, vol. 186, pp. 1-10, 1995.
9. FLUENT, Fluent, Inc., Lebanon, New Hampshire, 1998.
10. Foley, T. and Levy, A., "The erosion of heat-treated steels", Wear, vol. 91, pp. 45-64, 1983.
11. Gandhi, B.K., Singh, S.N., and Seshadri, V., "Study of the parametric dependence of erosion wear for the parallel flow of solid-liquid mixtures", Tribology International, vol. 32, pp. 275-282, 1999.
12. Golcar, G.R., Brooks, K.P., Darab, J.G., Davis, J.M., and Jagoda, L.K., "Development of inactive high-level waste envelope D Simulant for scaled crossflow filtration testing", Battelle Pacific Northwest National Laboratory Report No. PNWD-3042, 2000.
13. Graf, W. H., *Hydraulics of Sediment Transport*, McGraw-Hill Book Company, New York, 1971.
14. Hisamitsu, N., Iseh, T., and Takeishi, Y., "An experimental study on pipe erosion by sand slurry", Proc. 6th Conference on Slurry Transportation, Slurry Transport Association, pp. 319-332, 1981.
15. Iwai, Y. and Nambu, K., " Slurry wear properties of pump lining materials", Wear, vol. 210, 211-219, 1997.

16. Masayuki, T., Norio, K., Shozaburo, S., and Siro, M., "Hydraulic Conveying of Solids thruough Pipe Bends", J. of Chemical Engineering of Japan, vol. 5, No. 1, pp. 4-13, 1972.

17. Mills, D. and Mason, J.S., "Conveying velocity effects in bend erosion", J. Pipelines, vol. 1, pp. 9-81, 1981.

18. Mishra, A. and Finnie, I., "On the size effect in abrasive and erosive wear", Wear, vol. 65, pp. 359-373, 1981.

19. Neilson, J. H. and Gilchrist, A., "An analytical and experimental investigation of the velocities of particles entrained by the gas flow in nozzles", J. of Fluid Mech., vol. 33, pp. 131-149, 1968.

20. Roco, M.C. and Cader, T., "Energy approach for wear distribution in slurry pipelines", Jap. Journal of Multiphase Flow, vol. 4, pp. 2-20, 1990.

21. Roco, M.C and Minani, L.K., "Effect of particle size distribution and gravitation on wear in centrifugal pump castings", ASME Paper No. 89-FE8, 1989.

22. Shook, C.A. and Roco, M.C., *Slurry Flow*, Publ. Butterworth-Heinemann, 1991.

23. Singh, T., Tiwari, N., and Sundararajan, G., "Room temperature erosion behaviour of 304, 316, and 410 stainless steels", Wear, vol. 145, pp. 77-100, 1991.

24. Smith H.D. and Elmore, M.R., "Corrosion studies of carbon steel under impinging jets of simulated slurries of neutralized current acid waste (NCAW) and neutralized cladding removal waste (NCRW)", Battelle Pacific Northwest National Laboratory Report No. PNL-7816 (also UC-721), January 1992.

25. Zhong, Y. and Minemura, K., "Measurement of erosion due to particle impingement and numerical prediction of wear in pump casing", Wear, vol. 199, pp. 36-44, 1996.

26. Kay, J. M. and Nedderman, R. M., Fluid Mechanics and Transfer Processes, Cambridge University Press, Cambridge, 1985.

27. Ting, K. and Ma, Y. P., The Evaluation of Erosion/Corrosion Problems of Carbon Steel Piping in Taiwan PWR Nuclear Power Plant", Nuclear Engineering and Design, vol. 191, pp. 231-243, 1999.

28. W. M. Kays and M. E. Crawford, *Convective Heat and Mass Transfer*, Second Edition, McGraw-Hill Book Company, New York, 1980.

29. Humphrey, J. A. C., "Fundamentals of Fluid Motion in Erosion by Soli Particle Impact", Int. J. of Heat and Fluid Flow, vol. 11, No. 3, pp. 170-195, 1990.

30. Newitt, D. M., Richardson, J. F., Abbott, M., and Turtle, R. B., "Hydraulic Conveying of Solids in Horizontal Pipes", Tans. Instn Chem. Engineers, vol. 33, pp. 93-113, 1955.

31. Lee, S. Y. and Dimenna, R. A., "Validation Analysis for the Calculation of a Turbulent Free Jet in water Using CFDS-FLOW3D and FLUENT (U)", WSRC-TR-95-0170, May 1995.

32. H. Schlichting, Boundary Layer Theory, McGraw-Hill Book Company, New York, 1967.

33. W. M. Rohsenow and H. Y. Choi, *Heat, Mass, and Momentum Transfer*, Prentice-Hall, Inc., New Jersey, 1961.